Article

A 2-year calorie restriction intervention may reduce glycomic biological age biomarkers – a pilot study

Check for updates

Tea Pribić[1], Jayanta K. Das[2], Lovorka Đerek[3], Daniel W. Belsky[4], Melissa Orenduff[5], Kim M. Huffman[5], William E. Kraus[5], Helena Deriš[1], Jelena Šimunović[1], Tamara Štambuk[1], Azra Frkatović-Hodžić[1], Virginia B. Kraus[5], Sai Krupa Das[6], Susan B. Racette[7], Nirad Banskota[8], Luigi Ferrucci[2], Carl Pieper[9], Nathan E. Lewis[10], Gordan Lauc[1,11] & Sridevi Krishnan[12] ✉

In this pilot study, a subset of CALERIE Phase 2 (No. NCT00427193, registered 25th Jan 2007) participants ($n = 26$) were evaluated for the effects of 2 years of 25% calorie restriction (CR) on N-glycosylation of IgG, plasma, and complement C3, as well as IgG-based biological age (GlycAge). Plasma samples were collected at baseline (BL), 12 (12mo), and 24 months (24mo). IgG galactosylation was higher at 24mo compared to BL ($p = 0.051$) and increased from 12mo to 24mo ($p = 0.016$); GlycAge decreased over the same period ($p = 0.027$). GlycAge was positively associated with TNF-α ($p = 0.030$) and ICAM-1 ($p = 0.017$). Between BL and 24mo, plasma high-branched glycans declined ($p = 0.013$), bisecting GlcNAcs increased in both plasma ($p < 0.001$) and IgG ($p = 0.01$), complement C3 protein ($p < 0.001$), C3-Man9 ($p < 0.001$), and C3-Man9Glc1C3 ($p = 0.046$) were reduced. The absence of a control group warrants cautious interpretation.

Calorie restriction (CR), a dietary intervention involving a reduction in energy intake below the amount consumed ad libitum, delays aging and increases maximum lifespan in various species[1,2]. Animal studies suggest that CR could extend lifespan and slow aging; however, there are limited data in human populations, and gaps and inconsistencies in our understanding of the mechanisms by which CR is geroprotective[3–6]. Thus, newer mechanisms influencing aging are important to investigate, as they might elucidate human-specific pathways at play[6].

One potential contributing mechanism is protein N-glycosylation, a post-translational modification. Protein N-glycosylation is crucial to protein folding, stability, and function[7]. Further, with age, protein glycosylation is altered, and these alterations have been linked to various aging-related diseases, such that aberrant N-glycosylation may contribute to aging-related diseases via inflammaging and disruption of proteostasis[8–10].

A key example of aging-related glycosylation is alterations in the glycosylation of IgG. IgG is the predominant antibody (or immunoglobulin) produced by B cells, key players in cellular immunity. With aging, both chronic antigen stimulation and oxidative stress[11,12] upregulate inflammatory responses, leading to chronic low-grade inflammation, or inflammaging, a hallmark of aging[13]. With aging, IgG glycosylation changes include reductions in galactosylation and sialylation[14–19] and increases in bisecting N-acetylglucosamines (GlcNAc)[20–22]. These aging-related IgG glycosylation alterations are all pro-inflammatory via structural changes that promote an inflammatory response[14–19]. Thus, IgG glycosylation alterations are a result of and accelerate the age-related onset of chronic inflammatory disease. Leveraging this, the IgG N-glycome composition and its changes have been used to develop a biological age marker/index[23]. Furthermore, mono and di-galactosylated IgG glycans (but not agalactosylated IgG) and reduced

[1]Genos Ltd, Glycoscience Research Laboratory, Zagreb, Croatia. [2]Longitudinal Studies Section, Translation Gerontology Branch, National Institute on Aging, National Institutes of Health, Baltimore, MD, USA. [3]Clinical Department for Laboratory Diagnostics, University Hospital Dubrava, Zagreb, Croatia. [4]Robert N Butler Columbia Aging Center and Department of Epidemiology, Columbia University Mailman School of Public Health, New York, NY, USA. [5]Duke Molecular Physiology Institute and Department of Medicine, Duke University School of Medicine, Durham, NC, USA. [6]Jean Mayer, USDA, Human Nutrition Research Center on Aging at Tufts University, Boston, MA, USA. [7]College of Health Solutions, Arizona State University, Phoenix, AZ, USA. [8]Computational Biology and Genomics Core, National Institute on Aging, National Institutes of Health, Baltimore, MD, USA. [9]Division of Biostatistics, Department of Biostatistics and Bioinformatics, Duke University School of Medicine, Durham, NC, USA. [10]Departments of Pediatrics and Bioengineering, University of California, San Diego, CA, USA. [11]Faculty of Pharmacy and Biochemistry, University of Zagreb, Zagreb, Croatia. [12]School of Nutritional Sciences and Wellness, BIO5, University of Arizona, Tucson, AZ, USA. ✉e-mail: skrishnan@arizona.edu

bisecting GlcNAc's have been negatively associated with incident type 2 diabetes and cardiovascular disease[24–28].

While not as extensively studied as IgG glycosylation, glycosylation of complement C3 has recently come to be associated with metabolic and autoimmune diseases[29,30]. C3 is a component of the complement cascade, a critical arm of the innate immune system. Greater concentrations of C3 have been noted in metabolic disorders such as adiposity, dyslipidemia, insulin resistance, liver dysfunction, and diabetes, suggesting C3 may be a cardiometabolic risk factor[31,32]. Alternatively, lower C3 plasma concentrations have been tied to longevity in centenarian populations[33]. Aging-related changes in complement C3 include greater amounts of mannose-rich (high-mannose) and high-mannose glucosylated (such as GlcNAc2Mannose9Glucose1) glycans. These specific changes are associated with the onset of type 1 diabetes and renal complications arising from type 1 diabetes, both of which are hypothesized to be triggered by Endoplasmic Reticulum (ER) stress[30,34]. It is important to note that GlcNAc2Mannose9Glucose1 is involved in the process of initiating the unfolded protein response (UPR), which can trigger ER stress[35]. Elevated ER stress signals loss of proteostasis, another hallmark of aging[36,37], implicating a role for these specific glycoforms in the aging process.

In addition to immune-related glycoproteins like IgG and complement C3, total plasma protein glycome is also linked to age-related disease mechanisms[14]. Longitudinal investigations have identified the relative stability of the total plasma protein N-glycome over several years, while also identifying potential age-related changes[38]. Changes in plasma protein glycosylation patterns, such as appropriate sialylation and galactosylation, mark familial longevity and reflect healthy aging[39]. Moreover, several plasma, serum, and cell surface glycoprotein profiles in human epidemiological, animal model, and in vitro studies have identified agalactosylation and asialylation signatures, which have now come to be called "glycan" hallmarks of aging[14].

This manuscript outlines results from a pilot investigation focused on identifying changes in glycomic biomarkers of aging and age-related disease onset in response to a 2y CR intervention in healthy adults with normal weight or mild-moderate overweight (by BMI) from the Comprehensive Assessment of Long-term Effects of Reducing Intake of Energy (CALERIE™) trial. Specifically, IgG, C3, and total plasma protein N-glycosylation were evaluated. We further explored associations between CR-induced changes in a glycome-based biological age clock and epigenetic age clocks. Finally, we investigated muscle transcriptomic changes that are indicative of changes in glycosylation after the 2y CR intervention. Based on our understanding of glycomic changes resulting from aging[17] and chronic metabolic disease onset[14] we expected CR to favorably alter IgG and plasma protein N-glycosylation profiles with increased galactosylation and sialylation and reduced branching and bisecting GlcNAc. We expected CR to alter complement C3 glycosylation with fewer mannosylated and glucosylated C3

glycoforms. Furthermore, we anticipated that these alterations in the N-glycome would correlate with improvements in other biomarkers of aging, such as inflammation and epigenetic age clocks. Understanding the effect of CR on the glycome is crucial for advancing aging biology, and this study offers valuable data that could shape future investigations and interventions.

Results

In the 26 participants included in this pilot study, % CR was ~18% in the BL-12mo interval, and went down to ~9% in the 12–24mo interval (Fig. 1). Body weight reduced significantly between BL and 12mo, and increased slightly from 12 to 24mo.

CR effects on IgG GlycAge

A comparison of the chronological age of participants in this cohort (25.6–49.9 y at baseline - BL) and their calculated GlycAge is presented in Fig. 2. At 12mo, GlycAge was not different from chronological age, but at 24mo, GlycAge was lower than chronological age (Fig. 2A). A comparison of the slopes of a linear regression fit between GlycAge and chronological age against months in study (BL-12mo and 12–24mo) identified that the slope of GlycAge change between 12 and 24mo was significantly different from that of chronological age, but not between BL-12mo. Mean GlycAge (Fig. 2B) decreased between 12mo and 24mo ($p = 0.027$) but not between BL and 12mo or between baseline and 24mo. However, there was large inter-individual variability that warrants further investigation. During the BL-12mo interval (when the GlycAge change tracked chronological age), change in body weight was inversely associated with change in GlycAge; however, in the 12–24mo interval (when GlycAge was reduced in response to the intervention), there was no association between body weight change and GlycAge change.

In summary, GlycAge remained similar to chronological age at 12 months but was significantly lower at 24 months, with a notable decline between 12 and 24 months, independent of body weight change. Details of all outcomes from this report are tabulated in Supplementary Table 3, which includes Cohen's $f2$, while Supplementary Table 4 has other effect size metrics for mixed models presented here.

CR effects on the IgG N-glycome

Compared to 12mo, IgG di-galactosylation was greater at 24mo ($p = 0.039$). Compared to BL, total galactosylation (which is the sum of glycan structures with single and double galactoses- Fig. 3C) was greater at 24mo ($p = 0.051$). While there was no significant change in agalactosylation (i.e., glycan structures with no galactose sugars, Fig. 3D, $p = 0.073$), bisecting GlcNAc was higher at both 12mo and 24mo compared to BL ($p < 0.001$ and 0.019, respectively, Fig. 3E).

Fig. 1 | Anthropometric and calorie restriction characteristics of a subset of study participants ($n = 26$, 13 male, 13 female) are included in this report. **A** A line chart with points depicts body weight at baseline, 12mo and 24mo. **B** A box and whisker plot, with a dotted line separating the individual 12mo intervals from the total study %CR. The plots depict %CR during each intervention period. Inset p-values in (**A**) were obtained from repeated-measures mixed models with time (months) as the repeated measure and participant as a random effect. Inset p-values in (**B**) were obtained from repeated-measures mixed models using time intervals as repeated measures and participant as a random effect.
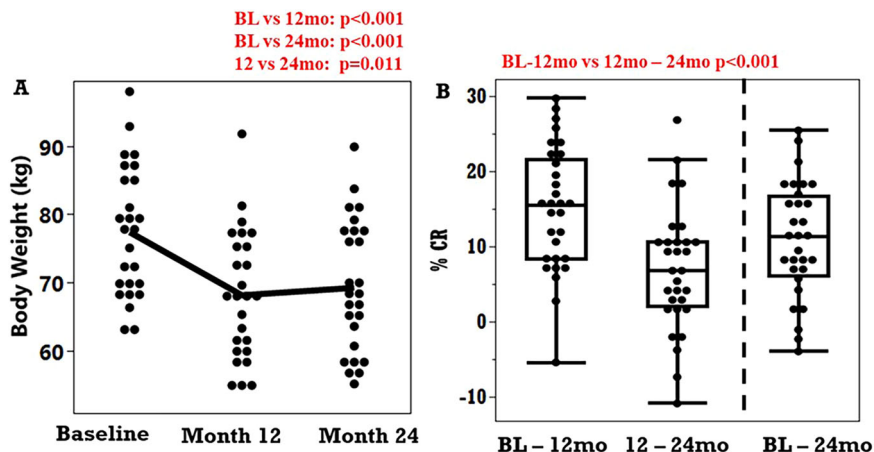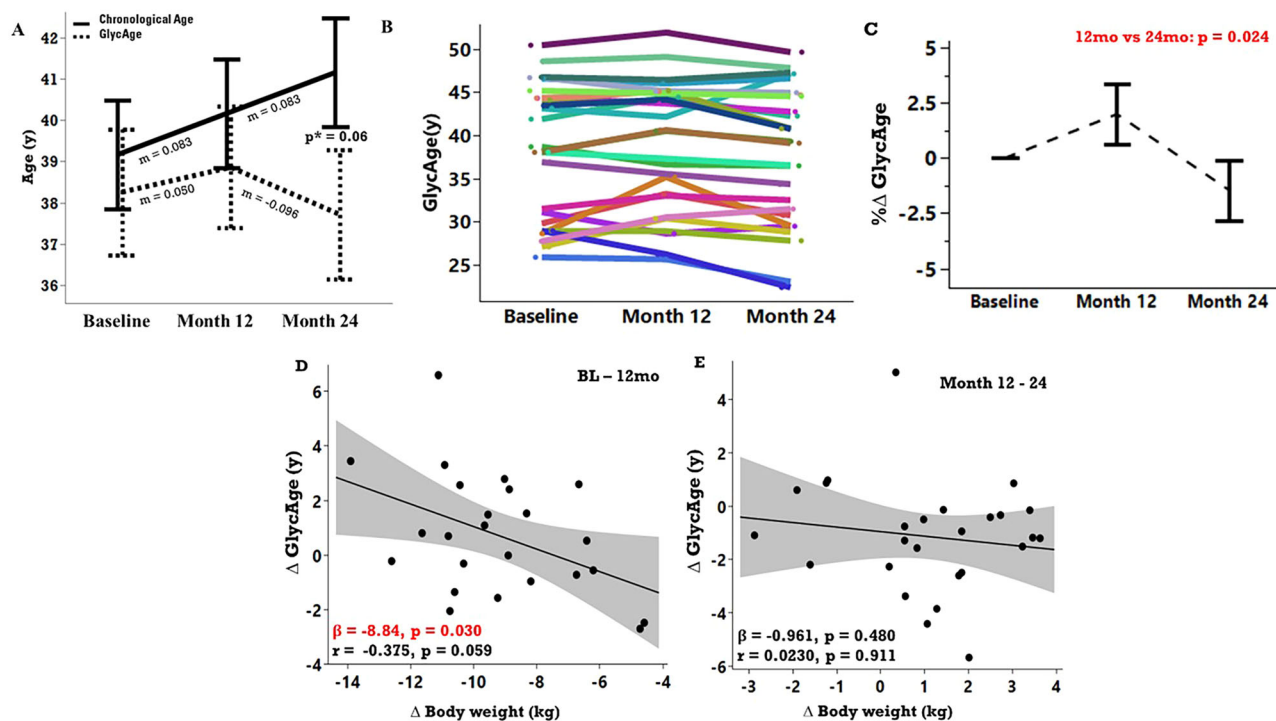
Fig. 2 | IgG glycosylation-based biological age - GlycAge - changes significantly in response to the CR intervention. A Chronological age compared to IgG-based biological age (GlycAge), with the slope (m) of each time interval (0–12mo and 12–24mo) inset, which were different ($p = 0.009$). However, a multiple comparison test (Tukey's) comparing the two ages indicated that at 24mo the two ages showed a difference of moderate significance ($p = 0.06$). **B** GlycAge for all participants in study – each line represents each participant, connecting dots measured at BL, 12mo, and 24mo. **C** Biological age (GlycAge) percent change from baseline with significant p-value inset. Differences were evaluated using a mixed model using visit month as a repeated measure, participant as a random effect, sex, and baseline GlycAge as covariates, followed by FDR correction. If the FDR corrected p-values were significant, multiple comparison tests (Tukey's) were conducted. Tukey's tests indicated that the 12mo–24mo ages were different ($p = 0.027$). **D, E** Change from baseline visit to 12mo and 12–24mo of IgG-based biological age GlycAge and change in body weight. Bivariate regression plots are shown with the β-estimate and corresponding p-value, and Spearman's correlation coefficient and corresponding p-values, inset evaluating the relationship between change in body weight and GlycAge by time interval (BL-12mo and 12–24mo).

In summary, IgG di-galactosylation and total galactosylation increased at 24 months, while bisecting GlcNAc was higher at both 12 and 24 months compared to baseline, though agalactosylation showed no significant change.

CR effects on total plasma N-glycome

Changes in select plasma glycome features before and after the 2y CR are presented in Fig. 4. Of particular interest are (a) highly sialylated and highly galactosylated glycans, both typically reduced with aging and chronic inflammation, (b) highly branched glycans, usually found at greater concentrations in chronic inflammatory diseases, and (c) glycans with bisecting GlcNAc, predominantly originating from immunoglobulins, which are also known to increase with biological age and chronic inflammation[14]. At 24mo, concentrations of tetra-sialylated glycans were reduced compared to BL ($p < 0.001$) and 12mo ($p = 0.031$). On the other hand, asialylated glycans were higher at 24mo compared to BL ($p = 0.011$) and 12mo ($p = 0.036$).

From BL to 24mo, there was an increase in agalactosylated glycans ($p = 0.019$), a reduction in tetra-galactosylated ($p = 0.021$) and highly branched glycans ($p = 0.013$). There was also an increase from BL to 12- and 24mo in bisecting GlcNAcs ($p < 0.001$, and $p = 0.013$, respectively). High-mannose glycans (HM) were also higher at 24mo compared to 12mo ($p = 0.035$).

In summary, following 2 y of caloric restriction, tetra-sialylated and highly branched glycans decreased, while asialylated and agalactosylated glycans increased; bisecting GlcNAcs rose at both 12 and 24 months, and high-mannose glycans were higher at 24 months.

CR effects on complement C3 N-glycome

Compared to baseline, at 12 and 24mo, complement C3 protein concentrations were significantly lower ($p < 0.001$, $p < 0.001$ respectively, Fig. 5).

Among the C3-Asn85 glycoforms (glycosylated at the 85th Asparagine residue), compared to baseline, the Man5 (Asn85 N2H5) glycoform was reduced at 24mo ($p = 0.002$) and the Man6 (Asn85 N2H6) glycoform was elevated at 24mo ($p < 0.001$). The Man7 (Asn85 N2H7) glycoform was lower at 12mo compared to baseline ($p < 0.001$) and higher at 24mo compared to 12mo ($p < 0.001$). Among the C3-Asn-939 glycoforms (glycosylated at the 939th Asparagine residue), compared to baseline, at 12mo and 24mo, the Man8 glycoform (Asn-939 N2H8) was greater ($p < 0.001$, $p = 0.034$ respectively), while Man9 (Asn-939 N2H9) was reduced at 12mo ($p < 0.001$) and 24mo ($p = 0.009$). Compared to baseline, Man9Glc1 (Asn-939 N2H10: Glucose1Mannose9GlcNAc2) glycoforms were decreased at 12mo and 24mo ($p = 0.015$, $p = 0.046$, respectively).

In summary, complement C3 protein levels were significantly lower at 12 and 24 months, with distinct changes in its glycoforms: Man5 decreased and Man6 increased at 24 months, while Man7 fluctuated over time; at Asn-939, Man8 increased, Man9 decreased, and Man9Glc1 was reduced at both time points.

Association between GlycAge and other epigenetic clocks

Using this subset of $n = 26$, Fig. 6A, B depicts a comparison of chronological age to previously published epigenetic[40] and non-epigenetic[41] clock/biological age data from CALERIE2, along with the GlycAge index. Non-epigenetic clocks included KDM (Klemera–Doubal Method) Biological Age, PhenoAge, and HD (Homeostatic Dysregulation), three methods to quantify biological aging using blood chemistry and clinical data[41]. KDM Biological Age estimates the chronological age at which an individual's physiology would be considered normal, and a KDM age that's higher than chronological age indicates faster aging, and a lower than chronological age indicates slower biological aging. PhenoAge, on the other hand, predicts the

Fig. 3 | IgG N-glycome changes in CALERIE2 participants. A A representative CGE-LIF electropherogram of IgG N-glycome, with graphic representation of glycan structures corresponding to each glycan peak (P). **B–E** show the percentage change from baseline in the IgG glycome among a subset of CALERIE2 study participants ($n = 26$). Data were evaluated by mixed models using visit month as a repeated measure, participant as a random effect, baseline values for each parameter, sex, and age as covariates, followed by FDR correction. If the FDR corrected p-values were significant, multiple comparison tests (Tukey's) were conducted. Significant p-values (inset in red) were obtained from Tukey's tests.
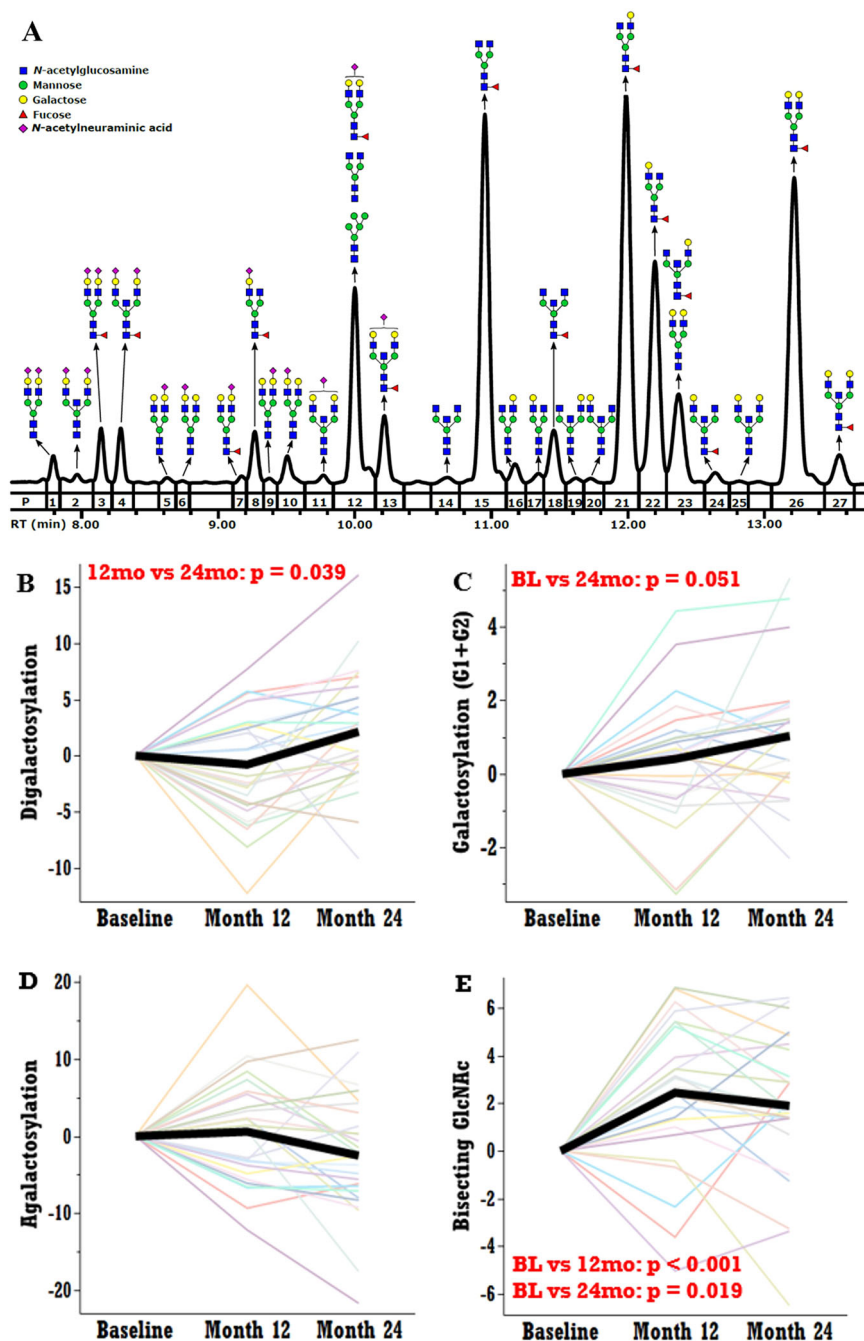
chronological age at which an individual's mortality risk would be typical in a reference population. PhenoAge higher than chronological age suggests greater/faster biological aging. Finally, Homeostatic Dysregulation (HD) measures how different an individual's physiology is from a healthy reference group, with higher values indicating more advanced biological aging.

While PC-GrimAge (an epigenetic clock) appears to increase with CR, DunedinPACE (also an epigenetic marker that measures pace of ageing) appears to decrease, like HD score and IgG GlycAge (these were not tested for significance). While all the epigenetic age clocks were positively correlated with each other (Fig. 6C) and with chronological age, IgG GlycAge, DunedinPace, and the non-epigenetic age clocks were not. Further, IgG GlycAge was inversely associated with both PC-GrimAge and PC-Skin and Blood Clocks, the latter both principal component-based versions of the original epigenetic clock ages – GrimAge[42] and Skin and Blood Clocks[43].

Associations between GlycAge and immune/metabolic parameters

Repeated measures correlation analysis revealed that GlycAge was significantly positively correlated with TGF-β, ICAM1, PDGF-AB, and TNF-α, while being inversely associated with HOMA-B (Fig. 7A–E). In mixed models where change in GlycAge was evaluated with the addition of inflammatory biomarkers as covariates, GlycAge sustained its significant difference between 12 and 24mo with TNFα as covariate (GlycAge $p = 0.030$, TNFα $p = 0.606$) and with ICAM1 as covariate (GlycAge $p = 0.014$, ICAM1 $p = 0.016$), but not with TFGβ as covariate (GlycAge $p = 0.181$, TFGβ $p = 0.183$).

Skeletal muscle transcriptomic changes in glycosylation processes due to CR

Figure 8 shows transcriptional changes in skeletal muscle glycogenes; CALERIE2 global DGE data were previously reported[44]. Compared to BL, at

Fig. 4 | Effect of 24mo CR on plasma N-glycome evaluated by mixed model tests using visit month as repeated measure, participant as random effect, baseline parameters, sex, and age as covariates, followed by FDR correction. If the FDR corrected *p*-values were significant, multiple comparison tests (Tukey's) were conducted, and significant *p*-values, if any, were highlighted in red. All figures show percent change from baseline. **A**, **B** Non-sialylated glycans were higher, whereas tetra-sialylated glycan species were lower at 24mo compared to BL. **C**, **D** Non-galactosylated species increased significantly, while tetra-galactosylated glycans reduced in the 12–24mo period of CR. **E** High-mannose glycans were significantly higher at 24mo compared to 12mo, but not compared to BL. **F** Glycans, with bisecting GlcNAc on plasma proteins, were higher at 12mo and 24mo compared to BL. **G** High-branched glycans were, however, lower at 24mo compared to BL.
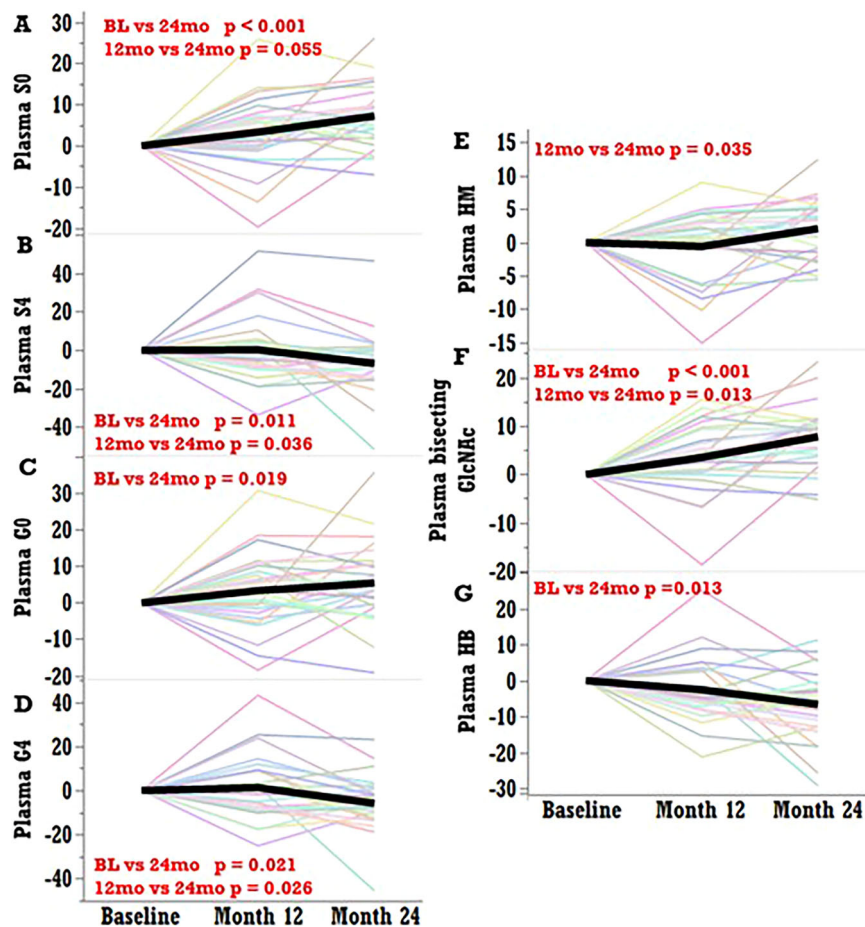
24mo, muscle expression was greater for CHST3, a heparan sulfate processing enzyme ($p < 0.01$) and HSPA5 an ER resident Hsp70 chaperone[45] involved in UPR ($p < 0.05$) (Fig. 8A). The largest number of differentially expressed genes in glycogene-related processes occurred in the ER and Golgi body, as expected, since the ER and the Golgi apparatus are responsible for most glycosylation processes (Fig. 8B). While N- and O-glycosylation processes were only ~1% of the total changes observed, glycosaminoglycans (GAGs) were ~9%.

Discussion
In this pilot study of 26 participants who underwent 24 months of CR, detailed glycosylation profiling indicates CR increased IgG galactosylation, reduced high-branched and highly sialylated glycans in plasma, reduced complement C3 protein levels, and affected several high-mannose and glucosylated C3 glycans, along with a reduction in GlycAge. Furthermore, GlycAge changes were associated with a few other established inflammation- and aging-related biomarkers, demonstrating the potential of glycans in assessing the impact of CR on biological ageing (a summary is provided in Supplementary Table 5). In addition, it is possible to speculate that the skeletal muscle transcriptome changes could have resulted from CR's impact on the ER at the transcriptional level. Specifically, after 2 y of CR, skeletal muscle expression of HSPA5, the binding immunoglobulin protein coding gene (involved in UPR), was upregulated.

With CR, GlycAge, an IgG-glycan-based biological age clock, was reduced from 12mo to 24mo, during the period of weight stability. GlycAge was not associated with epigenetic clock ages. However, in this subset of 26 participants, none of the examined epigenetic clocks were reduced by CR intervention, except for DunedinPACE, which approximates a pace of aging[40]. Consistent with an inflammaging biomarker[46], GlycAge was positively associated with various inflammatory biomarkers

(TGFβ1, TNFα, PDGF-AB, and ICAM1), which are known to increase with age and aging-related diseases[47]. CR also led to an increase in IgG galactosylation, an IgG-glycan feature usually associated with younger age and IgG's anti-inflammatory potential[48]. Surprisingly, an increase in IgG bisecting GlcNAc was also observed, a feature usually associated with increased pro-inflammatory IgG potential[21], which increases with aging[49]. This suggests that while some aging-related changes in the glycome are affected by CR, others may not be, or perhaps need a greater percentage of CR.

Our findings are consistent with others, where extensive weight loss induced by a 3-week low-calorie diet, followed by bariatric surgery, has been shown to alter IgG glycosylation and reduce inflammaging[50]. In the DIOGENES study[51] (*n* = 1850), the 8-week weight loss period reduced IgG agalactosylation, but did not affect galactosylation. However, at the end of the 6-month weight maintenance period, there was an increase in IgG di-galactosylation and an increase in bisecting GlcNAc. Similarly, in the CALERIE2 study, the initial baseline – 12mo period, when the weight loss was maximal (~−10kg), IgG di-galactosylation and GlycAge did not change significantly, but did change during the 12mo to 24mo period, when weight loss was minimal (~+0.5). While the %CR in the 12–24mo period recorded was lower, there was still substantial CR observed in the study population[52] and in this cohort, as observed in Fig. 1B, which shows the average CR during the entire 24mo duration. As noted earlier, % CR decreased within the first 20 weeks (5 months) of intervention, and continued to drop till 60 weeks (15 months), when it plateaued. Body weight also continued to decline till about 60 weeks, and then plateaued, reaching a new energy balance equilibrium during the 12–24mo period[52]. Thus, it is likely that the changes we observe in di-galactosylation and the GlycAge during the 12–24mo period are a function of achieving and maintaining this new equilibrium in energy balance.

Fig. 5 | Complement C3 changes due to intervention. Complement C3 concentration (**A**) and abundance of distinct C3 glycopeptides **B–D** glycosylated at asparagine (Asn)-85, and **E–G** glycosylated at Asn-939) before and after the 2y CR protocol in CALERIE2. All box plots show concentrations of total protein C3 and relative abundance of C3 glycopeptides at baseline, 12mo and 24mo of the CALERIE study in $n = 26$ participants. Data were evaluated using mixed models with visit month as a repeated measure, participant as a random effect, baseline values, sex, and age as covariates, followed by FDR correction. If the FDR corrected p-values were significant, multiple comparison tests (Tukey's) were conducted, and significant p-values, if any, were highlighted in red.
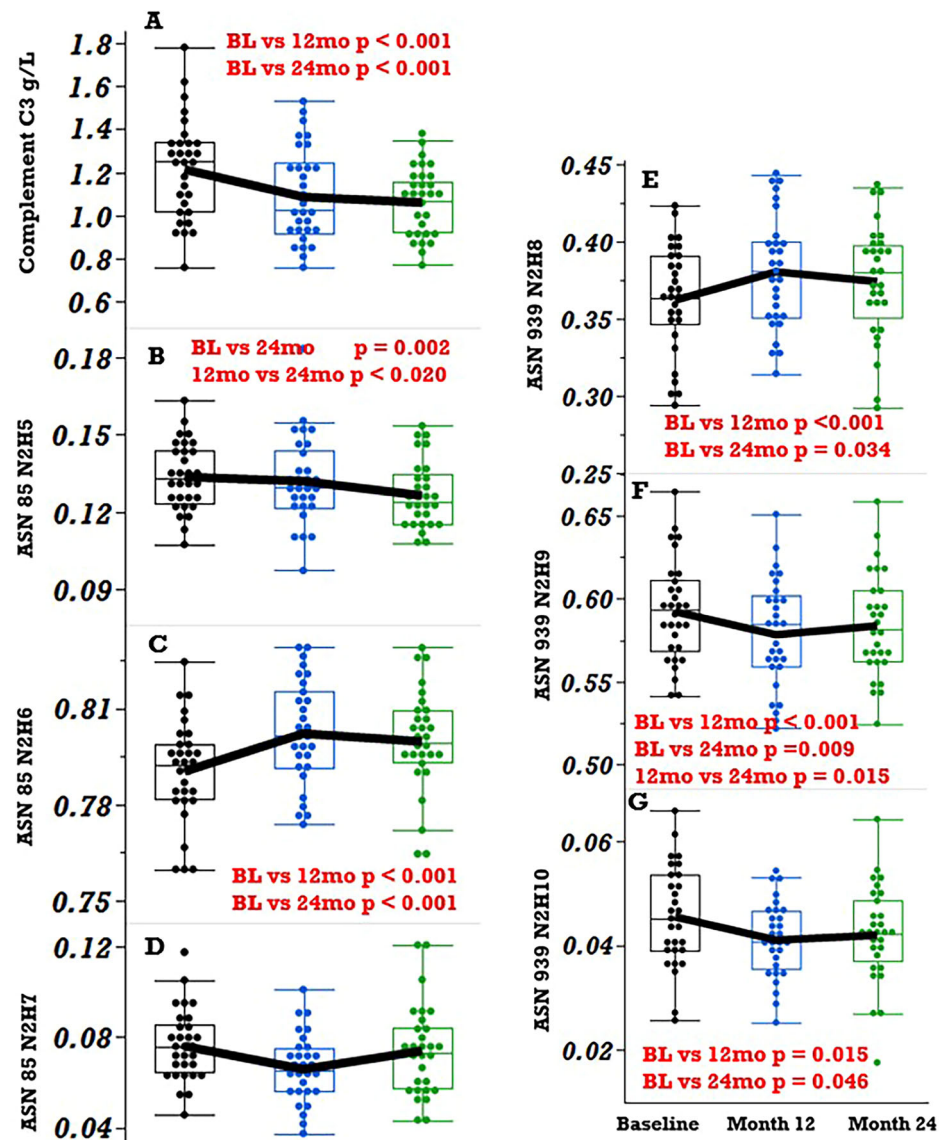
Glycosylation of total plasma protein, which includes several acute phase proteins, antithrombins, apolipoproteins, fibrinogens, and immunoglobulins[53] showed a decrease in highly sialylated and galactosylated structures following CR intervention, with concomitant increases in asialylated glycans. In addition, there were decreased levels of high-branched (tri-and tetra-antennary) glycans in circulation following the intervention. While glycosylation is cell and tissue-type-specific[54], plasma protein glycosylation patterns can provide overall insight into an individual's immune and metabolic status and can differentiate healthy vs certain diseased states[10,53]. The reduced branched and highly sialylated glycans are a beneficial change in plasma protein glycome, since high branching and high sialylation of N-glycans are associated with increased inflammation and have been implicated in the development of metabolic diseases[55–57]. The increase in asialylation and agalactosylation, indicative of increased biological aging[14] contrasts with the above findings. Hence, certain plasma glycome beneficial changes from the 2 y CR intervention were observed, while certain other biological aging-related processes were not.

Following the 2-year CR intervention, complement C3 concentrations decreased in the cohort we studied. Complement C3 is a critical component of innate and adaptive immunological processes and originates from hepatic and, occasionally, adipose tissue[58]. C3 concentrations are lower in naturally long-lived populations, e.g., centenarians, and higher in older individuals

with metabolic syndrome and abdominal obesity[33,59]. Based on these prior reports, our results suggest that CR reductions of complement C3 are indicative of improvements in metabolic health and aging processes.

The link between the complement C3 glycome and aging/metabolic diseases is less understood. Here, CR reduced levels of Man9 and Man9Glc1 C3 glycoforms. Complement C3 glycans have been reported to be more "unprocessed" (i.e., with more mannose and glucose residues) in individuals with higher hemoglobin A1c and uncontrolled glycemia-associated vascular complications, compared to healthy counterparts[30,34]. With 12 months of CR, the Man9 and Man9Glc1 glycoforms were reduced, with reductions continuing over 24 months for the Man9 glycans. The concurrent, 24 months increase in skeletal muscle expression of HSPA5, which encodes BiP, a UPR-associated chaperone, may indicate a means by which CR impacts ER stress through transcriptional and glycosylation processes to improve aging-related processes. CR upregulates chaperone proteins like HSPA5, which assist in protein folding and prevent the accumulation of misfolded proteins, maintaining proteostasis[60,61]. HSPA5 regulates apoptosis-related proteins, protecting cells from ER stress-induced apoptosis, indicating its cytoprotective role in maintaining cell viability[62]. Thus, in response to CR, the upregulation of HSPA5 likely serves as a protective mechanism to ensure proper protein folding, prevent apoptosis, and promote cell survival. This, in conjunction with the reduced Man9 and

Fig. 6 | Relationship between GlycAge and other biological age clocks in the n = 26 participants included in the current investigation. **A** Chronological age, IgG GlycAge, DNA methylation-based epigenetic clocks/ages (PC-GrimAge and DunedinPACE), and **B** non-epigenetic clocks (PhenoAge and HD score) at baseline, 12, and 24mo of the CR intervention. **C** A correlation matrix depicting repeated measures correlation coefficients between several epigenetic and non-epigenetic clock ages, IgG GlycAge, and chronological age at baseline, months 12 and 24. Any combinations of parameters not plotted (e.g., IgG GlycAge and HD.Clock), and all blank spaces did not have significant correlations; only *r* values with *p* < 0.05 are shown. Green indicates positive correlation, and red indicates negative correlation. PC – principal components.
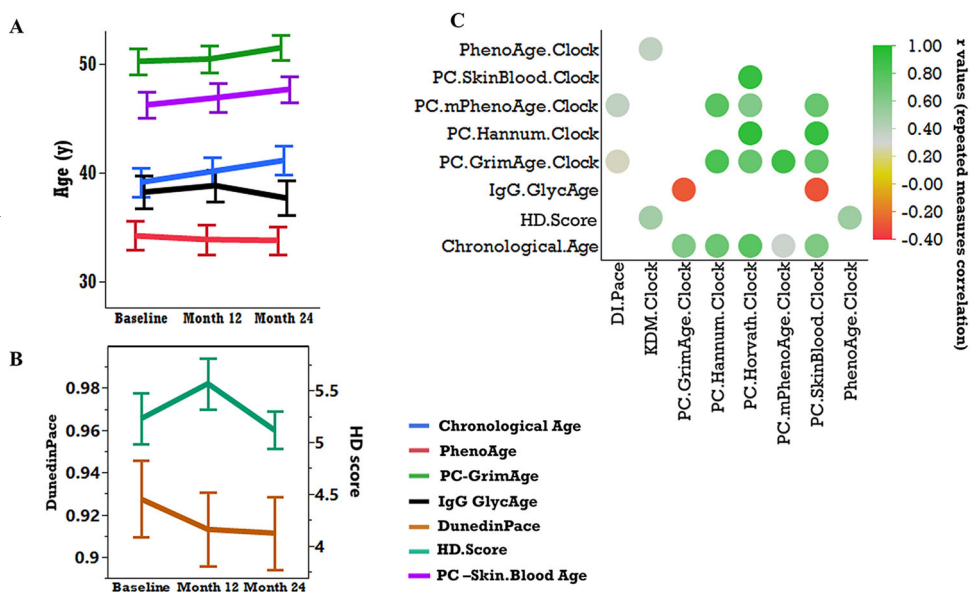
Fig. 7 | Correlation analysis between GlycAge, immune and metabolic parameters. A–E Repeated measures correlations (each color is one participant from n = 26) between GlycAge and immune parameters of interest at baseline, and 12 and 24mo of CR. Correlation coefficient r and corresponding *p*-values are shown, along with a repeated measures bivariate regression β-estimate and corresponding *p*-value.
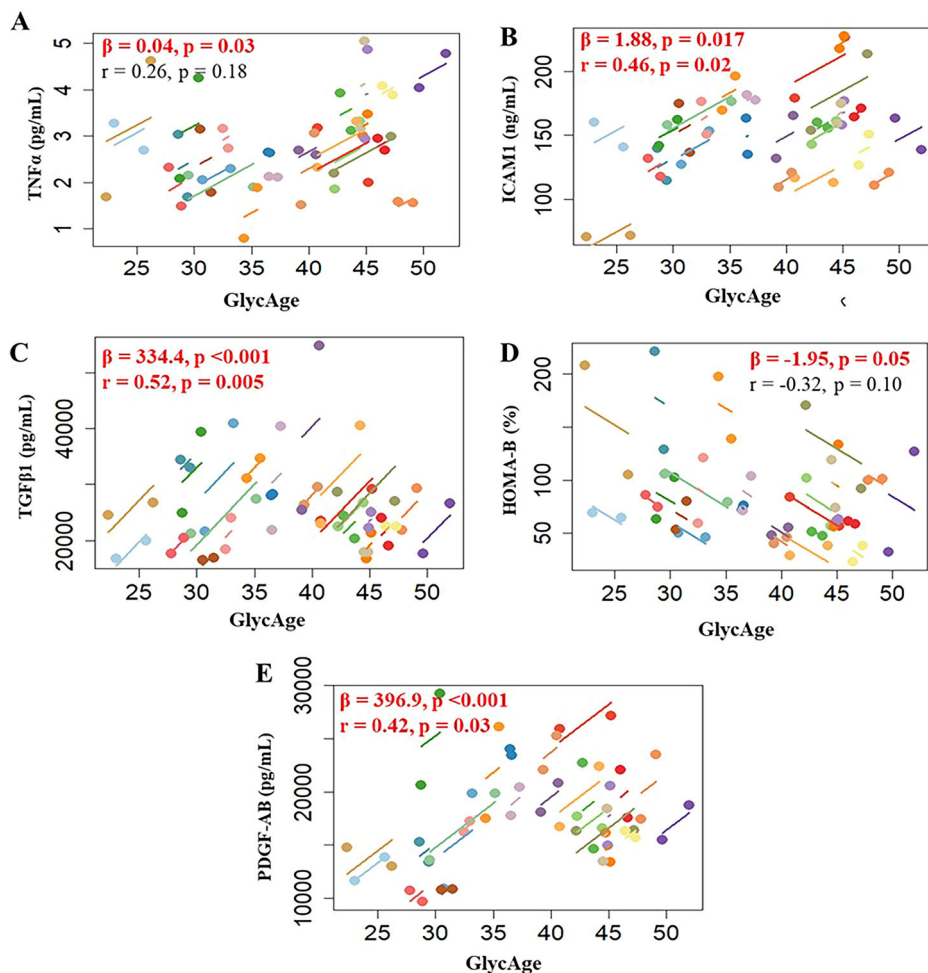
Man9Glc1 C3 glycans, hints at a potential mechanism by which CR influences ER stress, and which is reflected in the complement C3 glycome. However, given the lack of a control group, the small sample size, and the fact that the C3 originates from the liver, whereas the HSPA5 changes are observed in the skeletal muscle, this will remain a speculation until further investigations can elucidate this more definitively.

In conclusion, this was a pilot study limited due to its small sample size consisting of 26 out of 188 completers of the CALERIE2 trial, with an
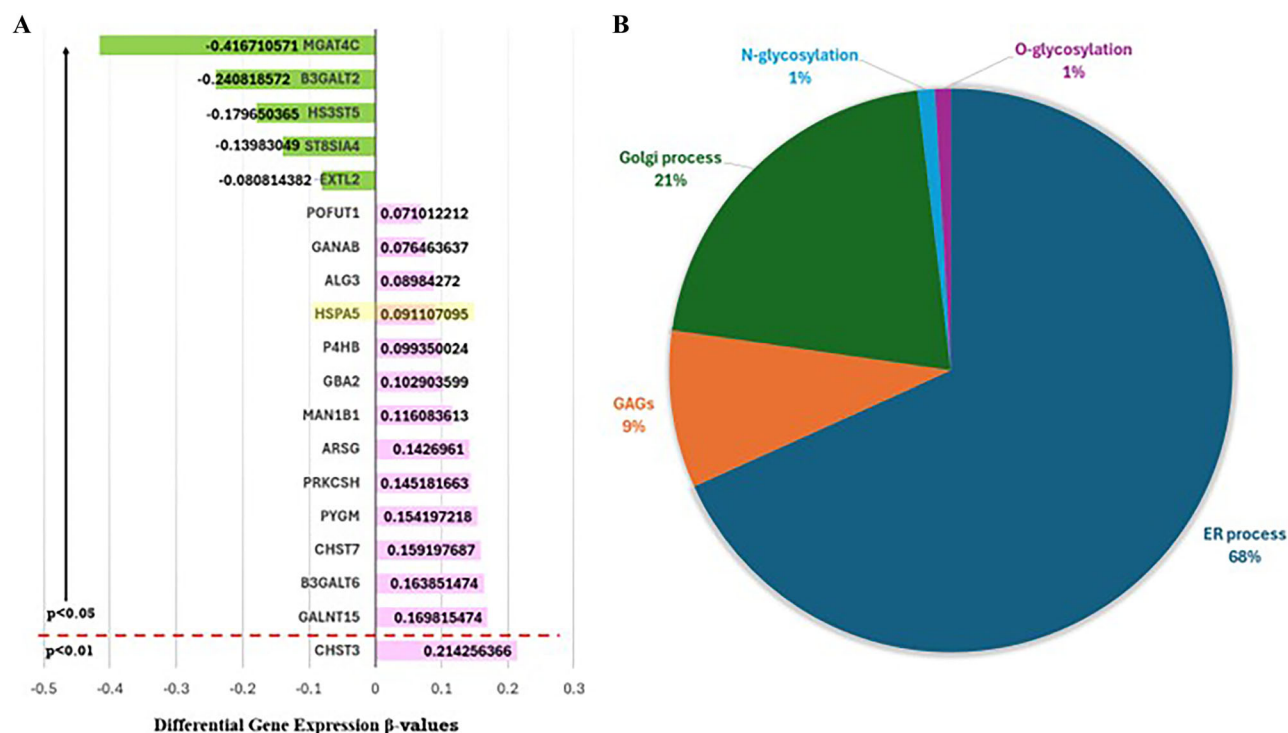
Fig. 8 | Differential gene expression analysis (DGE) of muscle (vastus lateralis) transcriptome data in $n = 90$ **(57 CR and 33 controls). A** shows glycogenes that were differentially expressed over the two-year CR (linear) at $p < 0.05$ threshold (CHST3 is the exception with a *p*-value of <0.01). The standardized beta values plotted and listed are positive if their expression was higher in CR at 24mo compared to baseline, and inverse if lower at 24mo compared to baseline. **B** depicts the percent of differentially expressed secretory pathway-related genes that are associated with different glycosylation processes, which are overexpressed in CR based on beta values in (**A**). GAGs – glycosaminoglycans/proteoglycans, ER endoplasmic reticulum.

average of >10% CR attainment at 12mo. Furthermore, we only studied the glycome of individuals in the CR group without comparison to the *ad libitum* group. This can introduce several biases including selection, compliance and attrition biases (we chose individuals with a high %CR, which may not represent the true distribution of CR maintained in the whole study, and does not account for attrition) and interpretation bias (lack of a control group can inflate positive findings in the intervention group, and potential confounding by time-varying factors that cannot be accounted for). The range-scaling step involved in the GlycAge calculation creates additional complexity compared to an ideal plug-and-play formula. Hence, future studies will aim to expand the cohort such that deeper insights with reduced bias can be obtained. Despite these limitations, our findings suggest that glycosylation biomarkers may play a key role in aging and inflammation, warranting further biochemical, genetic, cellular, and animal studies evaluation and validation. Such analyses might reveal diagnostic and therapeutic glycan targets that are useful in monitoring and manipulating biological age. Glyco-engineered IgG proteins, which have desired glycosylation profiles (i.e., more sialylated, more galactosylated, etc.), are being investigated as anti-inflammatory and anti-autoimmune therapeutics[63]. These might also have anti-aging benefits, and our ability to glyco-engineer therapeutics relies on being able to better understand the effect of CR on the glycome.

Methods
Study design
Details of the CALERIE Phase 2 trial were reported previously[64] and experimental design and protocols are archived on the website of the CALERIE Biorepository (https://calerie.duke.edu/sites/default/files/2022-05/phase2_protocol.pdf). Briefly, this multi-center randomized controlled trial included 220 participants randomized in a 2:1 ratio in favor of CR or to an *ad libitum* (AL) control group[64]. CR group participants were provided with an intensive behavioral intervention and were prescribed an intake 25%

below their total daily energy expenditure (which was equal to their energy intake at baseline). Participants' daily energy expenditure was estimated using doubly labeled water for four weeks at baseline, and subsequent time points to estimate %CR[65].

Participants
The study protocol (No. NCT00427193, registered 25th Jan 2007) received approval from the Institutional Review Boards of three clinical sites — Washington University Medical School (St. Louis, MO), Pennington Biomedical Research Center (Baton Rouge, LA), and Tufts University (Boston, MA) — as well as from the coordinating center at Duke University (Durham, NC). All study participants gave written informed consent. For this pilot investigation, we selected 26 participants from the CR group who completed the trial and who achieved the highest levels of CR (i.e., ~10–40% CR) on average.

Data and biospecimens from the biorepository
Plasma samples from the CALERIE2 study were obtained after approval from the CALERIE Steering Committee and the NIA Aging Research Biobank. De-identified plasma samples were recoded to blind the study personnel conducting analyses to the study time points. These samples are available from the NIA AgingResearchBiobank upon request (https://agingresearchbiobank.nia.nih.gov/studies/calerie/) and were obtained for baseline, 12mo, and 24mo. In addition, from the CALERIE Biorepository, we obtained anthropometrics (age, BMI, body weight, body composition), energy intake, energy expenditure and %CR, immune biomarkers (plasma TNF-α IL6, IL8, MCP1 (Monocyte chemoattractant protein-1), PDGF-AB (platelet-derived growth factor AB), TGFB1 (transforming growth factor – β1), CRP) and clinical variables (plasma HDL, LDL, triglycerides, total cholesterol, cortisol, fasting glucose and insulin, Homeostatic Model Assessment of Insulin resistance, HOMA-IR, Homeostasis Model Assessment of β-cell function (HOMA-β), Insulin-like growth factor binding

protein-1 and -3 (IGFBP1 and IGFBP3)) that were collected as part of the study. In addition, DNA methylation-based epigenetic clock information[40] and non-epigenetic clock/biological age measures[41] previously published (available for all $n = 26$ participants) were analyzed to evaluate associations with glycomic biological age measures. Finally, skeletal muscle transcriptome data published earlier[44] measured for $n = 75$ participants were also analyzed to identify glycosylation gene changes that were observed with the CR intervention.

Total plasma protein N-glycome analysis

For N-glycan release from total plasma proteins, each plasma sample (10 μL) was aliquoted into 1 mL 96-well collection plates (Waters, Milford, MA, USA) followed by a deglycosylation (release of glycans) procedure. Plasma proteins were denatured by the addition of 20 μl 2% (w/v) sodium dodecyl sulfate (SDS, Invitrogen, Carlsbad, CA, USA), and the sample was incubated at 65 °C for 10 min. After denaturation, 10 μl of 4% (v/v) Igepal-CA630 (Sigma–Aldrich, USA) was added to the samples, and the mixture was shaken for 15 min on a plate shaker (GFL, Germany). N-glycans were released by adding 1.2 U PNGase F (Promega, USA) and incubating overnight at 37 °C.

Fluorescent labeling and HILIC-SPE clean-up of released *N*-glycans

Released plasma N-glycans were labeled with 2-aminobenzamide (2-AB, Sigma–Aldrich). The labeling mixture consisted of 0.48 mg 2 AB and 1.12 mg 2-picoline borane (2-PB, Sigma–Aldrich) in 25 μl dimethyl sulfoxide (DMSO, Sigma–Aldrich) and glacial acetic acid (Merck, Darmstadt, Germany) (7:3, v/v) per sample. The labeling mixture was added to each sample, followed by incubation at 65 °C for 2 h. Excess reagents and proteins were removed from the samples using solid phase extraction by hydrophilic interaction liquid chromatography (HILIC-SPE) using 0.2 μm wwPTFE 96-well membrane filter plates (Pall, New York, NY, USA). The N-glycans were eluted with water and stored at −20 °C until use.

Hydrophilic interaction liquid chromatography of *N*-glycans

2AB-Fluorescently labeled glycans were separated on a Waters Glycan Premier BEH amide chromatography column, $150 \times 2.1\ mm \times 1.7\ \mu m$ BEH particles (Waters, USA), with 100 mM ammonium formate, pH 4.4 as solvent A and ACN as solvent B. A linear gradient of 30–47% ACN (Honeywell, USA) (v/v) at a flow rate of 0.561 ml/min was used for separation in a 32.5 min analytical run. The excitation and emission wavelengths were set to 250 nm and 428 nm, respectively. The chromatograms obtained were separated into 39 peaks (GP1-GP39) (Supplementary Fig. 1). The glycan peaks were analyzed by their elution positions and measured in glucose units, which were then compared to the reference values in the "GlycoStore" database (available at: https://glycostore.org/) for structure assignment[66,67]. The amount of glycans in each peak was expressed as a percentage of the total integrated area. For plasma glycans, 16 derived features were calculated in addition to 39 directly measured glycan features. (Supplementary Table 1).

Immunoglobulin G (IgG) N-glycome analysis

Samples were randomly distributed across three 96-well plates. To isolate IgG from a 25 μL plasma sample, the CIM® r-Protein G LLD 0.05 mL Monolithic 96-well plate (2 μm channels) (BIA Separations, Slovenia, Cat No. 120.1012-2) was used according to published protocols[17]. The vacuum-assisted setup utilized a manual system consisting of a multichannel pipette, a vacuum manifold (Pall Corporation, USA), and a vacuum pump (Pall Corporation, USA), with pressure reductions of approximately 5 mmHg during sample application and IgG elution. Following the isolation of IgG, the monolithic plate was stored in 20% (v/v) EtOH in 20 mM TRIS + 0.1 M NaCl, pH 7.4, at 4 °C. Subsequently, 20 μL of isolated IgG was aliquoted in a PCR plate (Thermo Scientific, UK) and dried in a vacuum centrifuge. For IgG N-glycan analysis by capillary gel electrophoresis with laser-induced fluorescence (CGE-LIF), deglycosylation, released N-glycan labeling, and

clean-up of labeled IgG N-glycans were performed using modified protocols described elsewhere[17,68].

IgG N-glycan release, labeling, and clean up

Isolated IgG samples were dried in a Savant SpeedVac vacuum concentrator, resuspended in 3 μL of 1.66 × PBS (w/v), and denatured in 4 μL 0.5% SDS (w/v) (Sigma–Aldrich, USA), followed by incubation at 65 °C for 10 min. Following incubation, 2 μL of 4% Igepal-CA630 (Sigma–Aldrich, USA) was added to the samples and incubated on a shaker for approximately 5 min. For glycan release, 1 μL of the enzyme mixture (1.2U of PNGase F (Promega, USA) in 1 μL 5× PBS) per sample was added and incubated for 3 h at 37 °C. After incubation, the deglycosylated IgG mix was dried in a vacuum concentrator for 1 h, diluted with 2 μL of ultrapure water, and left on a shaker for approximately 5 min to prepare the labeling mixture for labeling the released N-glycans. The labeling mixture was freshly prepared by combining 2 μL of 30 mM 8-aminopyrene-1,3,6-trisulfonic acid trisodium salt (APTS) (Synchem, DE) in 3.6 M citric acid (Sigma–Aldrich, USA) with 2 μL of 1,2 M 2-picoline borane in dimethylsulfoxide (Sigma–Aldrich, USA) per sample. Mixing was achieved by vortexing several times, followed by a 16 h incubation at 37 °C. The labeling reaction was stopped by adding 100 μL of cold 80% acetonitrile (Carlo Erba, Spain).

For the clean-up procedure, 200 μL of Bio-Gel P-10 slurry per well was added on a 0.2 μm wwPTFE AcroPrep filter plate (Pall Corporation, USA) and used as the stationary phase. The wells containing Bio-Gel P-10 were prewashed with 200 μL ultrapure water and 200 μL 80% cold ACN (v/v) (Carlo Erba, Spain), three times for each step. The samples were loaded into the wells and after a 5-min incubation on a shaker, samples were subsequently washed 5× with 5 × 200 μl 80% ACN containing 100 mM TEA, pH 8,5 (Carlo Erba, Spain/Millipore Sigma, USA) followed by 3 × 200 μl 80% ACN (Carlo Erba, Spain) after 2-min of incubation at room temperature. IgG N-glycans were eluted with a total of 500 μl of ultrapure water after 5-min incubation at room temperature after each step, and combined eluate fractions were stored at –20 °C until use.

Capillary gel electrophoresis N-glycan analysis and data processing

The IgG N-glycoprofiling by capillary gel electrophoresis with laser-induced fluorescence (CGE-LIF) was performed using an Applied Biosystems 3500 Genetic Analyser (Thermo-Fischer Scientific, USA), equipped with a 50-cm-long 8-capillary array (Thermo-Fischer Scientific, USA). Polymer POP-7 (Thermo-Fischer Scientific, USA) was used as a separation matrix in capillaries. In a 96-well MicroAmp Optical 96-Well reaction plate, 2 μl of APTS-labeled N-glycans were combined with 8 μl of HiDi formamide, ensuring a thorough and uniform resuspension. The instrumental method was created by setting the operating parameters as follows: injection time: 9 s; injection voltage: 15 kV; run voltage: 19.5 kV; oven temperature: 60 °C; and working time: 1000 s. The obtained electropherograms were integrated in the same manner into 27 peaks using Waters Empower 3 software. The Glycan composition of each peak has been previously determined[17]. For IgG glycans, 12 derived features were calculated in addition to 27 directly measured glycan peaks (Supplementary Table 2).

IgG-glycan-based biological age calculation

The IgG-glycan-based biological age index was developed previously by analyzing plasma glycome from ~5100 individuals from diverse populations using a linear gradient separation method[23]. In total, 906 individuals from the Croatian island Vis (377 men, 529 women), 915 individuals from the Croatian island Korcula (320 men, 595 women), 2035 individuals from the Orkney Islands in Scotland (797 men, 1238 women), and 1261 female twins from the TwinsUK cohort were measured. Their age ranges varied across cohorts, 16–100 years in Orkney, 18–98 in Korcula, 18–93 in Vis, and 27–83 in the TwinsUK cohort. The biological age index was developed as a function of specific galactosylated glycans (GP6, GP14, and GP15 – sialylated, mono and di-galactosylated low-branched glycans) and was found to explain a greater proportion of variance in biological age than telomere

length measures. In particular, the lesser galactosylated IgGs were identified to be a strong predictor of biological and chronological age, and inflammaging, while the more galactosylated versions reflected the opposite. These findings establish the IgG glycome as a marker of both inflammaging and aging-related diseases. Since its development, either the IgG-glycan-based biological age index or its chromatogram components (GPs) have been evaluated in various conditions, including diabetes[69], cardiovascular disease[70], rheumatoid arthritis[71], and neurodegenerative diseases[72], and demonstrated strong disease predictive capability. Using this[23,73], an IgG-glycan-based biological age (GlycAge) was calculated. Since the original formula was published, the IgG-based index has been made into a commercial product called GlycanAge, which uses a proprietary algorithm to calculate it[74]. As an alternative to the proprietary approach, we used a range-scaling step following the use of the formula, since the use of the formula alone returned values that did not resemble the age span for humans. The following formula (see Equation 1 below) was used as the final step in our analysis to ensure that GlycAge was within the range of the participants in the CALERIE2 study. While range-scaling is commonly used to scale data to a range between 0 and 1, it can also be applied to transform data into any other specified range. This is done by adjusting the data based on its minimum and maximum values, allowing it to be rescaled to a biologically relevant range or any other predefined limits.

$$\frac{(predicted\ GlycAge - Min\ of\ all\ predicted\ GlycAges) x (Max\ of\ CALERIE2age - Min\ of\ CALERIE2age)}{(Max\ of\ all\ predicted\ GlycAges - Min\ of\ all\ predicted\ GlycAges)}$$

Complement component (C3) N-glycome analysis

Complement component C3 was enriched from human plasma following the published method[34] with minor adjustments. Briefly, Concanavalin A (Con A)-Sepharose 4B resin (7.5 μL) was preconditioned with a binding buffer (20 mM Tris-HCl, 0.5 M NaCl, pH 7.4) on a 96-well polypropylene filter plate (Orochem Technologies Inc.). Plasma samples (10 μL) diluted with the binding buffer in a ratio of 1:9 were loaded on conditioned resin and incubated for 2 h at 4 °C, while shaking. Matrix was washed with 250 μL of binding buffer three times and incubated in 200 μL of elution buffer for 45 min before glycoproteins were eluted and dried in the vacuum concentrator.

C3 digestion and glycopeptide enrichment

Dried samples were resuspended in 78 μL of 15% (v/v) 2-propanol in 0.1 M ammonium acetate and denatured at 60 °C for 10 min. Subsequently, 2 μL of endoproteinase Glu-C (0.5 U/ μL) was added to samples for incubation overnight at 37 °C. Hydrophilic interaction chromatography-based solid phase extraction (HILIC-SPE) enrichment of glycopeptides was done as previously described[34] using 85% acetonitrile (ACN) instead of 90%.

Nano-LC-ESI-MS analysis

Enriched C3 glycopeptides were analyzed using an Ultimate 3000 RSLC nano system (Dionex/Thermo Fisher Scientific) coupled to an Orbitrap Exploris 240 (Thermo Fisher Scientific) using an EASY-Spray source. Samples (1 μL) were loaded onto an Acclaim PepMap C18 trap column (5 × 0.3 mm, 5 μm, 100 Å, Thermo Fisher Scientific) at a flow of 80 μL/min and washed for 3 min. Separation was performed on EASY-Spray PepMap™ RSLC C18 column (75 μm × 150 mm, particle size 3 μm, pore size 100 Å, Thermo Scientific) at a flow of 0.5 μL/min with a linear gradient. The column was maintained at 35 °C. The MS instrument was operated in a data-dependent mode. Samples were ionized at a spray voltage of 2250 V, and full MS1 scans were acquired within m/z 600–2000 with a 60,000 resolution and standard AGC target. The RF level was set to 90% and the maximum injection time was set to automatic. Previously annotated glycopeptides were separated based on the peptide backbone into two clusters with three glycoforms each (Supplementary Fig. 2). Data were extracted and quantified using LacyTools software[75].

Immunoturbidimetric C3 assay

The plasma concentration of complement C3 was measured using an immunoturbidimetric method with a commercial reagent kit (Beckman Coulter Inc., Brea, CA, USA) on the AU5800 Series Clinical Chemistry Analyzer (Beckman Coulter Inc., Tokyo, Japan) according to the Manufacturer's instructions. C3 from the sample reacts with the specific antibody from the reagent and forms insoluble complexes. The quantity of formed complexes is monitored spectrophotometrically, and the absorbance of the complex is proportional to the C3 concentration in the sample. The reference range was 0.79–1.52 g/L.

Statistical analysis

Data analyses were done using JMP Pro 17.2.0 (SAS Institute, Cary, NC) and R Statistical Software (R Studio version 2023.06.1, R version 4.3.1)[76]. All data were evaluated for normality and missingness. Data were transformed to log, cube root, or Johnson family of distributions (after evaluating several types of transformations) to achieve normality prior to analysis, evaluated using Q–Q plots (to evaluate linearity) and Shapiro–Wilk tests ($p > 0.05$). For anthropometric parameters, repeated measures mixed model analysis of covariance was used to evaluate the differences between baseline (BL), mid-intervention (12mo), and end of intervention (24mo) using participant as a random effect (Model 1). For all glycan parameters, repeated measures mixed model analysis of covariance was used to evaluate the differences in glycan parameters between baseline, 12mo, and 24mo. using participant as a random effect, baseline, age, and sex as covariates (Model 2), followed by FDR adjustment for multiple comparison correction. Where appropriate, family-wise multiple comparison tests (Tukey's) were performed to obtain individual time point differences. Bivariate regression with repeated measures, and repeated measures correlation (package rmcorr in R[77]) were used to evaluate relationships between glycan parameters and other features (epigenetic clocks from Waziry et al.ref. [40], non-epigenetic clocks from Kwon and Belsky[41] and immune and metabolic parameters) to account for repeated measures from the same individual at multiple time points. There was missing data in immune and metabolic parameters at baseline, and analyses in these instances were done using only available time points. To evaluate if the change in IgG GlycAge was independent of traditional inflammatory biomarkers, Model 1 was used, with the addition of inflammatory biomarkers as covariates one at a time (TNFα, TFGβ, ICAM1). Skeletal muscle differential gene expression (DGE) analysis was reported by Das et al., comparing 57 CR and 33 AL group individuals from the CALERIE2 trial. The DGE identified the top 1003 genes whose expression changed differentially between BL and 24mo at $p < 0.05$. Here, we further identified mammalian glycosylation genes (glycogenes) encoding glycosylation machinery enzymes as listed in the Glycoenzyme repository (https://glycoenzymes.ccrc.uga.edu/) that were among the 1003 identified genes from the DGE. Functional enrichment analysis using only the glycogenes was done with g:Profiler, which identified specific glycosylation processes that were different between the CR and AL groups.

Data availability

All data will be available from the AgingResearchBiobank (NIA) and the CALERIE2 repository at Duke.

References

1. Bales, C. W. & Kraus, W. E. Caloric restriction: implications for human cardiometabolic health. *J. Cardiopulm. Rehabil. Prev.* **33**, 201–208 (2013).
2. Fontana, L. & Klein, S. Aging, adiposity, and calorie restriction. *JAMA* **297**, 986–994 (2007).

3. Brown, J. E. Can restricting calories help you to live longer?. *Post Reprod. Health* **20**, 16–18 (2014).

4. Kaeberlein, M. et al. Regulation of yeast replicative life span by TOR and Sch9 in response to nutrients. *Science* **310**, 1193–1196 (2005).

5. Lopez-Lluch, G. & Navas, P. Calorie restriction as an intervention in ageing. *J. Physiol.* **594**, 2043–2060 (2016).

6. Most, J., Tosti, V., Redman, L. M. & Fontana, L. Calorie restriction in humans: an update. *Ageing Res. Rev.* **39**, 36–45 (2017).

7. Shental-Bechor, D. & Levy, Y. Effect of glycosylation on protein folding: a close look at thermodynamic stabilization. *Proc. Natl. Acad. Sci. USA* **105**, 8256–8261 (2008).

8. Zhang, J. et al. Type II epithelial-mesenchymal transition upregulates protein N-glycosylation to maintain proteostasis and extracellular matrix production. *J. Proteome Res.* **18**, 3447–3460 (2019).

9. Li, J., Zhang, D., Wiersma, M. & Brundel, B. Role of autophagy in proteostasis: friend and foe in cardiac diseases. *Cells* https://doi.org/10.3390/cells7120279 (2018).

10. Dotz, V. & Wuhrer, M. N-glycome signatures in human plasma: associations with physiology and major diseases. *FEBS Lett.* **593**, 2966–2976 (2019).

11. Ventura, M. T., Casciaro, M., Gangemi, S. & Buquicchio, R. Immunosenescence in aging: between immune cells depletion and cytokines up-regulation. *Clin. Mol. Allergy* **15**, 21 (2017).

12. Baylis, D., Bartlett, D. B., Patel, H. P. & Roberts, H. C. Understanding how we age: insights into inflammaging. *Longev. Healthspan* **2**, 8 (2013).

13. Franceschi, C., Garagnani, P., Parini, P., Giuliani, C. & Santoro, A. Inflammaging: a new immune-metabolic viewpoint for age-related diseases. *Nat. Rev. Endocrinol.* **14**, 576–590 (2018).

14. Paton, B., Suarez, M., Herrero, P. & Canela, N. Glycosylation biomarkers associated with age-related diseases and current methods for glycan analysis. *Int. J. Mol. Sci.* https://doi.org/10.3390/ijms22115788 (2021).

15. Ito, K. et al. Lack of galactosylation enhances the pathogenic activity of IgG1 but Not IgG2a anti-erythrocyte autoantibodies. *J. Immunol.* **192**, 581–588 (2014).

16. Terai, I., Kobayashi, K., Vaerman, J. P. & Mafune, N. Degalactosylated and/or denatured IgA, but not native IgA in any form, bind to mannose-binding lectin. *J. Immunol.* **177**, 1737–1745 (2006).

17. Pucic, M. et al. High throughput isolation and glycosylation analysis of IgG-variability and heritability of the IgG glycome in three isolated human populations. *Mol. Cell Proteom.* **10**, M111 010090 (2011).

18. Bosseboeuf, A. et al. Pro-inflammatory state in monoclonal gammopathy of undetermined significance and in multiple myeloma is characterized by low sialylation of pathogen-specific and other monoclonal immunoglobulins. *Front. Immunol.* **8**, 1347 (2017).

19. Campbell, I. K. et al. Therapeutic effect of IVIG on inflammatory arthritis in mice is dependent on the Fc portion and independent of sialylation or basophils. *J. Immunol.* **192**, 5031–5038 (2014).

20. Fukuta, K. et al. Control of bisecting GlcNAc addition to N-linked sugar chains. *J. Biol. Chem.* **275**, 23456–23461 (2000).

21. Ruhaak, L. R. et al. Decreased levels of bisecting GlcNAc glycoforms of IgG are associated with human longevity. *PLoS ONE* **5**, e12566 (2010).

22. Umana, P., Jean-Mairet, J., Moudry, R., Amstutz, H. & Bailey, J. E. Engineered glycoforms of an antineuroblastoma IgG1 with optimized antibody-dependent cellular cytotoxic activity. *Nat. Biotechnol.* **17**, 176–180 (1999).

23. Krištić, J. et al. Glycans are a novel biomarker of chronological and biological ages. *J. Gerontol. A Biol. Sci. Med. Sci.* **69**, 779–789 (2014).

24. Birukov, A. et al. Immunoglobulin G N-glycosylation signatures in incident type 2 diabetes and cardiovascular disease. *Diab. Care* **45**, 2729–2736 (2022).

25. Hoshi, R. A. et al. N-glycosylation profiles of immunoglobulin G and future cardiovascular events. *Circ. Res.* **134**, e3–e14 (2024).

26. Menni, C. et al. Glycosylation profile of immunoglobulin G is cross-sectionally associated with cardiovascular disease risk score and subclinical atherosclerosis in two independent cohorts. *Circ. Res.* **122**, 1555–1564 (2018).

27. Wu, Z. et al. IgG glycosylation profile and the glycan score are associated with type 2 diabetes in independent chinese populations: a case-control study. *J. Diabetes Res.* **2020**, 5041346 (2020).

28. Lemmers, R. F. H. et al. IgG glycan patterns are associated with type 2 diabetes in independent European populations. *Biochim. Biophys. Acta Gen. Subjects* **1861**, 2240–2249 (2017).

29. Rudman, N. et al. Integrated glycomics and genetics analyses reveal a potential role for N-glycosylation of plasma proteins and IgGs, as well as the complement system, in the development of type 1 diabetes. *Diabetologia* **66**, 1071–1083 (2023).

30. Soic, D. et al. Human complement component C3 N-glycome changes in type 1 diabetes complications. *Front. Endocrinol.* **14**, 1101154 (2023).

31. Hertle, E., van Greevenbroek, M. M. & Stehouwer, C. D. Complement C3: an emerging risk factor in cardiometabolic disease. *Diabetologia* **55**, 881–884 (2012).

32. Xu, C. et al. Serum complement C3 levels are associated with nonalcoholic fatty liver disease independently of metabolic features in Chinese population. *Sci. Rep.* **6**, 23279 (2016).

33. Fu, S. et al. Centenarian longevity is positively correlated with IgE levels but negatively correlated with C3/C4 levels, abdominal obesity and metabolic syndrome. *Cell Mol. Immunol.* **17**, 1196–1197 (2020).

34. Soic, D. et al. High-throughput human complement C3 N-glycoprofiling identifies markers of early onset type 1 diabetes mellitus in children. *Mol. Cell Proteom.* **21**, 100407 (2022).

35. Ware, F. E. et al. The molecular chaperone calnexin binds Glc1Man9GlcNAc2 oligosaccharide as an initial step in recognizing unfolded glycoproteins. *J. Biol. Chem.* **270**, 4697–4704 (1995).

36. Hipp, M. S., Kasturi, P. & Hartl, F. U. The proteostasis network and its decline in ageing. *Nat. Rev. Mol. Cell Biol.* **20**, 421–435 (2019).

37. Hartl, F. U., Bracher, A. & Hayer-Hartl, M. Molecular chaperones in protein folding and proteostasis. *Nature* **475**, 324–332 (2011).

38. Reiding, K. R. et al. High-throughput serum N-glycomics: method comparison and application to study rheumatoid arthritis and pregnancy-associated changes. *Mol. Cell Proteom.* **18**, 3–15 (2019).

39. Ruhaak, L. R. et al. Plasma protein N-glycan profiles are associated with calendar age, familial longevity and health. *J. Proteome Res.* **10**, 1667–1674 (2011).

40. Waziry, R. et al. Effect of long-term caloric restriction on DNA methylation measures of biological aging in healthy adults from the CALERIE trial. *Nat. Aging* **3**, 248–257 (2023).

41. Kwon, D. & Belsky, D. W. A toolkit for quantification of biological age from blood chemistry and organ function test data: BioAge. *Geroscience* **43**, 2795–2808 (2021).

42. Faul, J. D. et al. Epigenetic-based age acceleration in a representative sample of older Americans: Associations with aging-related morbidity and mortality. *Proc. Natl. Acad. Sci. USA* **120**, e2215840120 (2023).

43. Horvath, S. et al. Epigenetic clock for skin and blood cells applied to Hutchinson Gilford Progeria Syndrome and ex vivo studies. *Aging* **10**, 1758–1775 (2018).

44. Das, J. K. et al. Calorie restriction modulates the transcription of genes related to stress response and longevity in human muscle: the CALERIE study. *Aging Cell* **22**, e13963 (2023).

45. Malhotra, J. D. & Kaufman, R. J. Endoplasmic reticulum stress and oxidative stress: a vicious cycle or a double-edged sword?. *Antioxid. Redox Signal.* **9**, 2277–2293 (2007).

46. Shkunnikova, S. et al. IgG glycans in health and disease: prediction, intervention, prognosis, and therapy. *Biotechnol. Adv.* **67**, 108169 (2023).

47. Vatic, M., von Haehling, S. & Ebner, N. Inflammatory biomarkers of frailty. *Exp. Gerontol.* **133**, 110858 (2020).

48. Gudelj, I., Lauc, G. & Pezer, M. Immunoglobulin G glycosylation in aging and diseases. *Cell Immunol.* **333**, 65–79 (2018).

49. Stambuk, J. et al. Global variability of the human IgG glycome. *Aging* **12**, 15222–15259 (2020).

50. Greto, V. L. et al. Extensive weight loss reduces glycan age by altering IgG N-glycosylation. *Int. J. Obes.* **45**, 1521–1531 (2021).

51. Deris, H. et al. Effects of low-calorie and different weight-maintenance diets on IgG glycome composition. *Front. Immunol.* **13**, 995186 (2022).

52. Dorling, J. L. et al. Changes in body weight, adherence, and appetite during 2 years of calorie restriction: the CALERIE 2 randomized clinical trial. *Eur. J. Clin. Nutr.* **74**, 1210–1220 (2020).

53. Clerc, F. et al. Human plasma protein N-glycosylation. *Glycoconj. J.* **33**, 309–343 (2016).

54. Medzihradszky, K. F., Kaasik, K. & Chalkley, R. J. Tissue-specific glycosylation at the glycopeptide level. *Mol. Cell Proteom.* **14**, 2103–2110 (2015).

55. Rudman, N., Gornik, O. & Lauc, G. Altered N-glycosylation profiles as potential biomarkers and drug targets in diabetes. *FEBS Lett.* **593**, 1598–1615 (2019).

56. Mise, K. et al. Novel urinary glycan biomarkers predict cardiovascular events in patients with type 2 diabetes: a multicenter prospective study with 5-year follow up (U-CARE Study 2). *Front. Cardiovasc. Med.* **8**, 668059 (2021).

57. Cvetko, A. et al. Plasma N-glycome shows continuous deterioration as the diagnosis of insulin resistance approaches. *BMJ Open Diabetes Res. Care* https://doi.org/10.1136/bmjdrc-2021-002263 (2021).

58. Ricklin, D., Reis, E. S., Mastellos, D. C., Gros, P. & Lambris, J. D. Complement component C3 - The "Swiss Army Knife" of innate immunity and host defense. *Immunol. Rev.* **274**, 33–58 (2016).

59. Wu, N. et al. Proteomic characteristics of plasma and blood cells in natural aging rhesus monkeys. *Proteomics* **22**, e2200049 (2022).

60. Dos Santos, C. et al. Caloric restriction promotes beta cell longevity and delays aging and senescence by enhancing cell identity and homeostasis mechanisms. *Res. Sq.* https://doi.org/10.21203/rs.3.rs-3311459/v1 (2023).

61. Yang, L. et al. Long-term calorie restriction enhances cellular quality-control processes in human skeletal muscle. *Cell Rep.* **14**, 422–428 (2016).

62. Du, B. et al. MiR-30c regulates cisplatin-induced apoptosis of renal tubular epithelial cells by targeting Bnip3L and Hspa5. *Cell Death Dis.* **8**, e2987 (2017).

63. Mimura, Y. et al. Glycosylation engineering of therapeutic IgG antibodies: challenges for the safety, functionality and efficacy. *Protein Cell* **9**, 47–62 (2018).

64. Ravussin, E. et al. A 2-year randomized controlled trial of human caloric restriction: feasibility and effects on predictors of health span and longevity. *J. Gerontol. A Biol. Sci. Med. Sci.* **70**, 1097–1104 (2015).

65. Racette, S. B. et al. Approaches for quantifying energy intake and % calorie restriction during calorie restriction interventions in humans: the multicenter CALERIE study. *Am. J. Physiol. Endocrinol. Metab.* **302**, E441–E448 (2012).

66. Centers for Disease Control. National Diabetes Surveillance System: Division of Diabetes Translation (2024).

67. Zhao, S. et al. GlycoStore: a database of retention properties for glycan analysis. *Bioinformatics* **34**, 3231–3232 (2018).

68. Hanic, M., Lauc, G. & Trbojevic-Akmacic, I. N-glycan analysis by ultra-performance liquid chromatography and capillary gel electrophoresis with fluorescent labeling. *Curr. Protoc. Protein Sci.* **97**, e95 (2019).

69. Memarian, E. et al. IgG N-glycans are associated with prevalent and incident complications of type 2 diabetes. *Diabetes Metab. Res. Rev.* **39**, e3685 (2023).

70. Lim, S. Y. et al. N-glycan profiles of acute myocardial infarction patients reveal potential biomarkers for diagnosis, severity assessment and treatment monitoring. *Glycobiology* **32**, 469–482 (2022).

71. Pasek, M. et al. Galactosylation of IgG from rheumatoid arthritis (RA) patients–changes during therapy. *Glycoconj. J.* **23**, 463–471 (2006).

72. Lundstrom, S. L. et al. Blood plasma IgG Fc glycans are significantly altered in Alzheimer's disease and progressive mild cognitive impairment. *J. Alzheimers Dis.* **38**, 567–579 (2014).

73. Kristic, J., Lauc, G. & Pezer, M. Immunoglobulin G glycans - biomarkers and molecular effectors of aging. *Clin. Chim. Acta* **535**, 30–45 (2022).

74. GlycanAge. *How Our Biological Age Test Works* https://glycanage.com/how-it-works (2025).

75. Jansen, B. C. et al. LaCyTools: a targeted liquid chromatography-mass spectrometry data processing package for relative quantitation of glycopeptides. *J. Proteome Res.* **15**, 2198–2210 (2016).

76. R Core team. A language and environment for statistical computing. https://www.R-project.org/ (Vienna, Austria, 2021).

77. Jonathan, Z. & Bakdash, L. R. M. rmcorr: Repeated Measures Correlation. https://cran.r-project.org/web/packages/rmcorr/index.html (2023).

Acknowledgements

Author contributions

S.K., G.L. and N.E.L. conceived the study hypothesis, S.K. obtained regulatory approvals and samples from NIA; L.D. generated Complement C3 data; G.L., T.P., H.D., J.S., T.S., and A.F.H. generated all glycomic data; J.K.D., N.B., and L.F. generated transcriptomic data, D.W.B. generated DNA methylation and epigenetic age data; S.K., T.P., and A.F.H. conducted glycomic data analysis, J.K.D. and S.K. conducted transcriptomic data analysis of glycogenes; C.P. had significant input into statistical approaches utilized; S.K. conducted comparative analyses between epigenetic and glycomic data; M.O., K.M.H., W.E.K., V.B.K., S.K.D., S.B.R., and C.P. were involved in conceiving, designing and conducting the original CALERIE2 intervention and data analysis from that study; S.K. wrote the first draft, all authors read, offered critical input and reviewed the final version.

Competing interests

Additional information